IEEE Access
Multidisciplinary | Rapid Review | Open Access Journal

Received April 15, 2019, accepted April 22, 2019, date of publication May 2, 2019, date of current version May 15, 2019.

Digital Object Identifier 10.1109/ACCESS.2019.2914498

Evaluation of the Possible Use of PPG Waveform Features Measured at Low Sampling Rate

DAISUKE FUJITA AND ARATA SUZUKI
Faculty of Systems Engineering, Wakayama University, Wakayama 640-8510, Japan
Corresponding author: Arata Suzuki (aratas@sys.wakayama-u.ac.jp)

This work was supported by the JSPS KAKENHI under Grant JP16K00393.

ABSTRACT To date, the applications of photoplethysmograms in the estimation of cuff-less blood pressure, arteriosclerosis, and so on have been studied. Photoplethysmogram waveform features have often been used to estimate the target volumes. For these estimations, it is necessary to acquire photoplethysmogram waveforms and changes in their derivative waveform details, for which the photoplethysmograms measured at comparatively high sampling rates have been used. The performance of smartphone cameras and wearable photoplethysmogram sensors has improved; with regard to mobile health technology, photoplethysmograms measured at lower sampling rates offer considerable advantages. These include lower computational resources, compression of accumulated data, and lower sensor power consumption. However, compared to photoplethysmograms measured at a high sampling rate, photoplethysmogram measurement at a low sampling rate will result in waveform signal degradation. This paper investigates the possibility of using photoplethysmograms measured at a low sampling rate. To this end, we statistically compared photoplethysmogram waveform features obtained from 63 male subjects free of circulatory diseases, at a sampling rate of 240 Hz, with waveform features obtained at low sampling rates (120, 60, 30, 20, and 10 Hz) through downsampling, and evaluated possible commercial use.

INDEX TERMS Big data, mobile health, photoplethysmogram, waveform feature.

I. INTRODUCTION

According to a WHO report, approximately 70% of worldwide deaths in 2015 are estimated to be due to lifestyle diseases [1]. Generally, lifestyle diseases take time to progress and are ultimately linked, in many cases, to serious illnesses, such as cerebral stroke and myocardial infarction. Daily monitoring of physical and mental health is expected to lead to an awareness of health and an improvement in lifestyle habits. Mobile devices such as smartphones and smart watches have been increasingly used in improving physical and mental health. Health management technology using these types of mobile devices is known as ''mobile health,'' and the development of health apps for smartphones has received considerable attention [2]–[5].

Mobile devices used for mobile health enable various types of biodata to be obtained [6], [7]. The biodata acquired using mobile devices is useful for the user's own health management; in addition, this biodata aggregated from many users can be obtained as big data [8], [9]. Of the biological signals obtainable from mobile devices, photoplethysmograms (PPGs) are particularly easy to use. PPGs are signals of blood volume changes near the body's surface measured by camera and light sensors such as photodiodes [10], [11]. The degrees of freedom in the measured regions are high, since PPGs can acquire data from the face, fingertips, and wrists. They can also be used in physical and mental health assessments, since they include information on circulatory and autonomic nerve functions. Autonomic nerve evaluations derived from heartbeat measurement and heart rate variability (HRV) are examples of PPG use with mobile devices [12]–[14]. These measurements are used for electrocardiogram (ECG) RR intervals and correlated pulse intervals (PI) [15], [16]. PI consist of valley-to-valley intervals of PPGs, determined without the need for detailed PPG waveform shapes in a single pulse. It is possible to stably acquire HRV features using PI from PPGs at relatively low sampling rates [17].

PPGs are not used only for heart rate measurement; owing to recent popularity of mobile health, PPGs have been used in evaluations of circulatory health. Research into arterial stiffness has reported on age, vasoactive drugs, diseases such

The associate editor coordinating the review of this manuscript and approving it for publication was Filbert Juwono.

as arteriosclerosis and diabetes, and changes in PPG waveforms [18]. Moreover, substantial research is being conducted on cuff-less blood pressure estimation using PPG waveform features [2], [19], [20]. To obtain detailed features from PPG waveforms, these research efforts used a dedicated sensor at a comparatively high sampling rate for PPG measurement.

On the other hand, in the mobile health field, there are several advantages to conducting PPG measurement at low sampling rates, such as reduced power consumption and computational resources. In addition, when collecting PPG big data, if the transmitted PPG data volume is limited, communication traffic will be reduced and database storage saved. However, since a reduced sampling rate may result in degraded PPG signals, the sampling rate should be lowered only to a level that does not affect the purpose of use. From the same perspective, while research exists on the effect of a lowered sampling rate on HRV [17], to the authors' knowledge, studies on the effect of a lower sampling rate on PPG waveform features used in the evaluation of circulatory functions have not been conducted to date. Therefore, this study investigated the influence of lower sampling rates on PPG features used in evaluating circulatory functions.

II. WAVEFORM FEATURES

Here, we explain the conventional relationship between PPG waveform features and various circulatory functions. To date, PPG waveform shapes have been quantified and various PPG waveform features proposed to evaluate targeted circulatory functions [21]. Evaluation of circulatory functions was possible through a detailed understanding of morphological changes in PPG waveform features. When abstracting PPG waveform changes, in order to clarify the PPG's inflexion and zero-crossing points, first and second derivative PPG waveforms are often used. These two derivative PPGs are known as FDPPG and SDPPG. However, research on FDPPG's waveform features is limited [21] compared to that on PPG's and SDPPG's waveform features. This study investigates features abstracted from PPG and SDPPG waveforms.

A. PPG WAVEFORM FEATURES

In general, PPG signals are decomposed into DC and AC components (Fig. 1(a)). It has been frequently reported that PPG's DC components reflect the subject's respiratory cycle [11]. The AC components carry pulse periodicity, including much data reflecting the status of the circulatory organs. Generally, a single-pulse PPG waveform characteristically consists of three peaks and valleys. These are called the systolic peak, dicrotic notch, and diastolic peak (Fig. 2). There are many cases of PPG waveform features using these values. The PPG waveform features used in this study are listed in Table 1. These features are often used in PPG applied research. However, we recommend consulting reference material for the detailed, physiological significance of these features.

Systolic peak, dicrotic notch, and diastolic peak are needed for acquisition of the many PPG waveform features listed in Table 1. However, very often, for PPG waveforms, data except for that of the systolic peak is unclear. There are many cases, in particular, of the dicrotic notch and diastolic peak

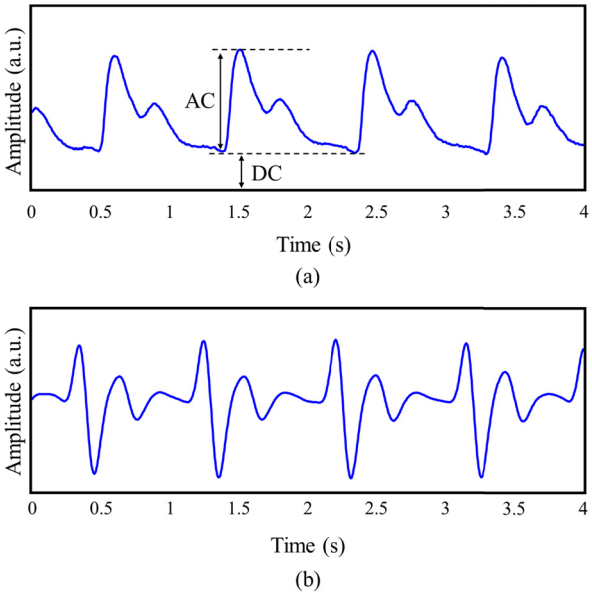

FIGURE 1. (a) Photoplethysmogram waveform, (b) second derivative photoplethysmogram waveform.

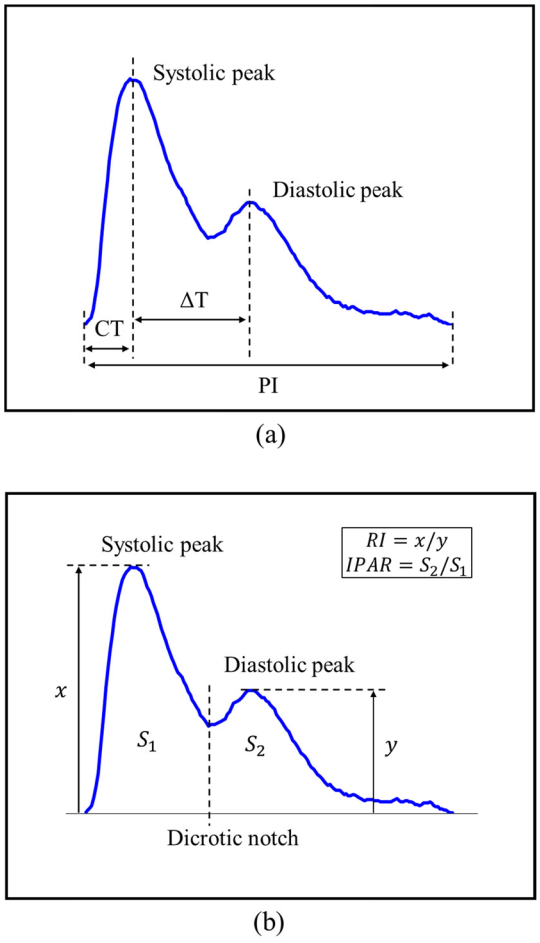

FIGURE 2. Single-pulse PPG and its waveform features, (a) time domain features, (b) other features.

TABLE 1. PPG waveform features used in this paper.

PPG characteristic	Function	Proposer	Sampling rate [Hz]
Pulse interval (PI)	Exercise effect	Poon *et al.* [16]	undescribed
Inflection point area ratio (IPAR)	Cardiac output	Wang *et al.* [22]	100
ΔT	Large artery stiffness	Millasseau *et al.* [23]	100
Crest time (CT)	Arterial stiffness	Alty *et al.* [24]	100
Augmentation index (AI)	Vascular aging	Takazawa *et al.* [18]	undescribed
	Arterial stiffness	Alty *et al.* [24]	100

TABLE 2. SDPPG waveform features used in this study.

SDPPG characteristic ratio	Function	Proposer	Sampling rate [Hz]
b/a	Arterial distensibility	Imanaga *et al.* [25]	undescribed
	Hypertension	Hashimoto *et al.* [26]	undescribed
	Framingham risk score	Otsuka *et al.* [27]	undescribed
c/a	Vasoactive agent effect	Takazawa *et al.* [18]	undescribed
	Vascular aging	Baek *et al.* [28]	500
d/a	Vasoactive agent effect	Takazawa *et al.* [18]	undescribed
	Hypertension	Hashimoto *et al.* [26]	undescribed
e/a	Vasoactive agent effect	Takazawa *et al.* [18]	undescribed

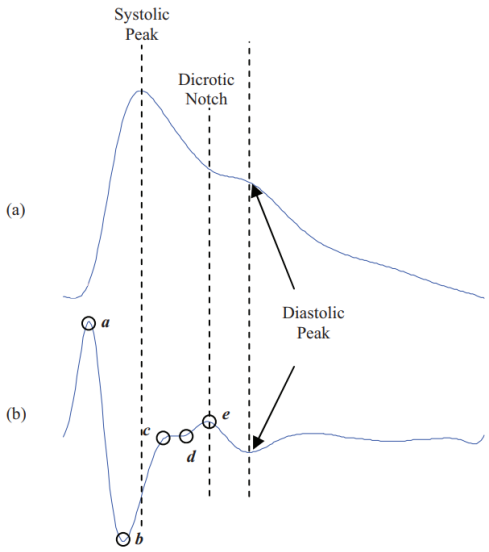

FIGURE 3. Method of determining the positions of the dicrotic notch and diastolic peak from a PPG waveform lacking clear definition of these data (Elgendi [21] Fig. 15).

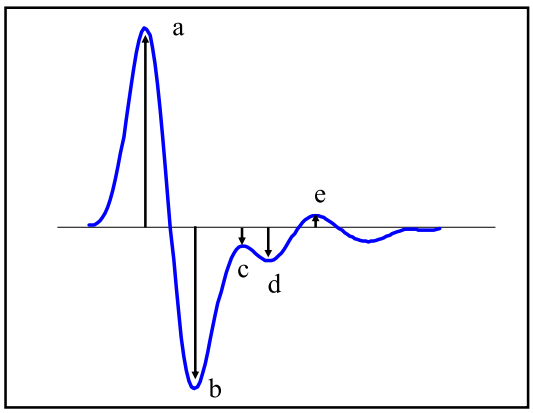

FIGURE 4. Single-pulse SDPPG waveform and its five peaks.

dissipating due to the effects of ageing and other factors. Derivative PPG is used to determine the dicrotic notch and diastolic peak in these PPG waveforms. An example is shown in Fig. 2 where the rise and fall of SDPPG is used to determine these data.

B. SDPPG WAVEFORM FEATURES

SDPPG waveforms have clear peaks and troughs, unlike PPG waveforms. In general, SDPPG waveforms have five characteristic peaks and valleys (Fig. 4). Their relationship to the various circulatory functions has been widely researched. In order of precedence, these five peaks and valleys are known, within a single-pulse SDPPG waveform, as a, b, c, d and e. The most basic method to characterize these is to measure the height of each wave, except a, from the baseline, and calculate a height ratio for each wave against wave a. Table 2 shows the height ratios used in this paper (b/a, c/a, d/a and e/a).

III. MATERIALS AND METHODS

A. PPG MEASUREMENT

The PPG sensor used in this experiment comprised of a red light source (wavelength: 660 nm) and a photodiode. Two-minute PPG measurements were taken using a 16-bit A/D converter at a 240 Hz sampling rate. Sixty-three males aged 38.6 ± 12.2 and with no history of circulatory disease participated in this experiment. We obtained the approval

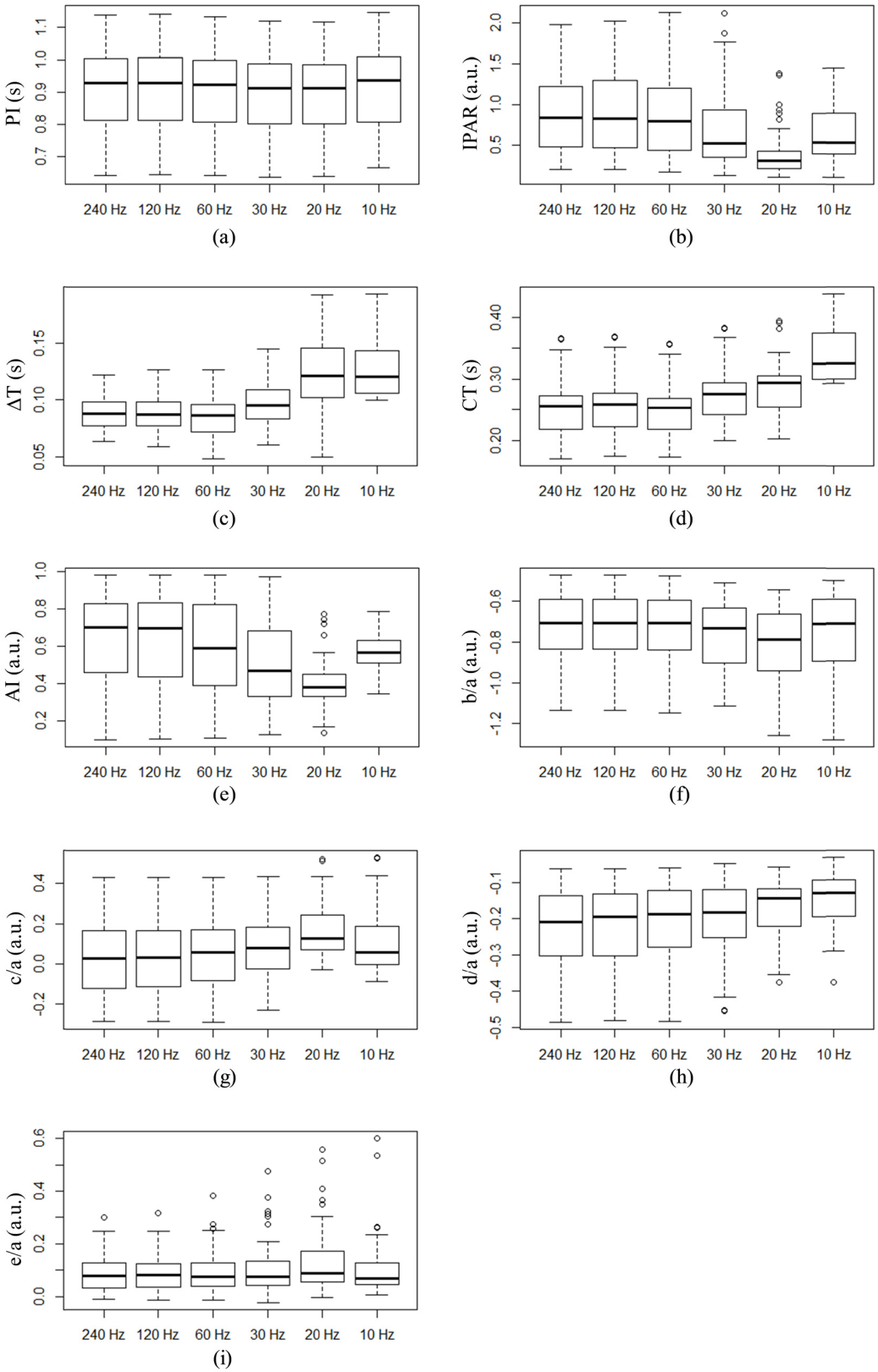

FIGURE 5. Box plot representation of the waveform features, (a) PI, (b) IPAR, (c) ΔT (d) CT, (e) AI, (f) b/a, (g) c/a, (h) d/a, and (i) e/a.

of the Ethics Committee at the Kanai Hospital and consent from the subjects (after explaining the experimental objectives and methods to them) and proceeded with measurement. The procedure involved PPG measurements from the tip of the left-hand index finger at 20° C, room temperature, with each subject in the seated position after 5 min of rest.

TABLE 3. Feature value variation rates determined through sampling, with the features at 240 Hz as reference.

PI

	Mean	SD	Max	Min
120 Hz	0.2	0.1	0.4	0.2
60 Hz	-5.2	0.1	-4.7	-5.4
30 Hz	-1.4	0.3	-0.8	-1.9
20 Hz	-1.7	0.5	0.6	-2.5

IPAR

	Mean	SD	Max	Min
120 Hz	1.3	4.2	8.2	-14.0
60 Hz	-4.7	14.5	24.3	-39.9
30 Hz	-19.8	27.7	38.8	-72.2
20 Hz	-49.6	27.3	24.1	-81.6

ΔT

	Mean	SD	Max	Min
120 Hz	-0.8	3.8	6.7	-13.0
60 Hz	-4.0	11.3	18.7	-47.1
30 Hz	10.7	16.4	55.6	-26.8
20 Hz	43.1	27.2	104.7	-42.2

CT

	Mean	SD	Max	Min
120 Hz	1.7	0.4	2.6	0.7
60 Hz	-0.6	1.1	1.6	-2.6
30 Hz	9.3	2.7	17.3	4.2
20 Hz	15.1	4.1	26.6	6.9

AI

	Mean	SD	Max	Min
120 Hz	-0.8	11.2	67.9	-47.7
60 Hz	-6.6	11.7	26.8	-42.2
30 Hz	-18.5	21.3	59.3	-67.8
20 Hz	-34.7	26.4	114.3	-62.9

b/a

	Mean	SD	Max	Min
120 Hz	0.1	0.2	1.8	-0.1
60 Hz	0.5	1.1	6.4	-1.4
30 Hz	4.8	3.5	13.4	-2.8
20 Hz	11.9	5.5	25.6	2.5

c/a

	Mean	SD	Max	Min
120 Hz	-5.0	52.8	112.7	-387.6
60 Hz	-16.6	200.8	765.8	-1318.2
30 Hz	-23.9	363.9	1813.5	-2086.5
20 Hz	-47.9	348.2	1556.1	-1933.7

d/a

	Mean	SD	Max	Min
120 Hz	-1.6	3.0	3.6	-13.6
60 Hz	-7.5	11.3	8.6	-45.4
30 Hz	-10.5	18.8	25.2	-57.3
20 Hz	-15.7	29.5	29.4	-71.7

e/a

	Mean	SD	Max	Min
120 Hz	7.3	51.6	408.1	-14.1
60 Hz	62.0	457.3	3629.3	-38.7
30 Hz	181.5	1256.1	9981.3	-51.9
20 Hz	615.7	4088.8	32515.9	-72.1

Unit: %

For PPG signal filtering, first a 16-order FIR low-pass filter with a cutoff frequency of 10 Hz was used. Then, a moving-average low-pass filter with the same cutoff frequency was used.

Low sampling rate PPG signals were acquired by down-sampling from a PPG signal measured at 240 Hz. For low sampling rates, frequencies of 120 Hz, 60 Hz, 30 Hz, 20 Hz, and 10 Hz were selected. Here, we explain the down-sampling method used in this study. First, the downsampling point interval d is determined using a low sampling rate, f_{low}.

$$d = \frac{240}{f_{low}} \tag{1}$$

Taking as candidates the start points of PPG downsampled at point d from the start point of the PPG measured at 240 Hz, the start points of downsampled PPG were randomly selected. Each of these start points were sampled at point d to obtain the respective low sampling-rate signals. Low sampling rate PPG signals were thus obtained via PPG signal downsampling

subjected to secondary derivation, and low sampling rate SDPPG signals were acquired.

Multiple pulses were contained in a single PPG record (2-min measurement), and features were abstracted from each pulse. To obtain highly reliable waveform features for each subject, their records were individually characterized as the average of features obtained from all PPG and SDPPG pulses per record. This average is calculated using the following formula when K individual features are acquired from a record created at the f_s Hz sampling rate.

$$average_{f_s} = \frac{1}{K}\sum_{i=1}^{K} featurevalue_i \tag{2}$$

When features for individual pulses were lost within the record, they were averaged for pulses without feature loss.

B. EVALUATION OF PPG FEATURE FLUCTUATION DUE TO LOW SAMPLING RATE

The sampling rate used in this study for PPG measurement was 240 Hz. Taking the abstracted features as reference, we confirmed the fluctuation in waveform features at a low sampling rate. With features acquired at 240 Hz as the reference points, the rate of feature change at low sampling rates is calculated as follows:

$$variation\ of\ average_{f_s}\% = \frac{average_{f_s} - average_{240}}{average_{240}} \times 100 \tag{3}$$

In addition, to confirm whether or not waveform feature statistical specificity is maintained, we analyzed the box plots for each feature.

IV. RESULTS

The rate of change of features at each low sampling rate, with 240 Hz as the reference point, is shown in Table 3. All features are shown in box plots in Fig. 5.

Much of the past research on PPG and SDPPG waveform features used a sampling rate of 100 Hz or higher. The results of this study show that, for any feature, there is little fluctuation in features when the sampling rate is changed from 240 Hz to 120 Hz. Table 3 shows high fluctuation rates for conditions when c/a and e/a exceed 100%. This could be because c/a and e/a tend to zero. The box plots of these features for 120 Hz show that there is no major change in statistical properties at this sampling rate. Even at 60 Hz, the same tendency is observed. At a 30 Hz sampling rate, most features fluctuate considerably, but CT, PI, and b/a variations are small. Because PI is calculated according to the inter-pulse valleys of a PPG waveform, it stabilizes and can be acquired. CT similarly stabilizes and is acquirable because it is calculated according to the inter-pulse valleys of a PPG waveform and the systolic peak. Additionally, since the SDPPG b wave is distinct, b/a also stabilizes and is acquirable. At 20 Hz and 10 Hz sampling rates, almost all features fluctuate considerably, but PI is stable.

V. CONCLUSION

In this study, features acquired from PPG measurement at 240 Hz and the fluctuation of features at low sampling rates of 120 Hz, 60 Hz, 30 Hz, 20 Hz, and 10 Hz. The nine feature types dealt considered in this study showed little fluctuation even down at a sampling rate of 60 Hz; these can therefore be considered commercially usable. However, at a sampling rate lower than 30 Hz, only some features can be considered commercially usable.

For future research using PPG waveform features and their targeted applications (heart rate measurement, blood pressure estimation, and vascular status estimation), the results will enable selection of an appropriate sampling rate for the selection of useful PPG waveform features.

As a research restraint, we mention here the use of a smartphone camera for PPG measurement. In this study, a 16-bit resolution PPG sensor was used to generate PPG signals, and not from a smartphone camera. If a smartphone camera is used for PPG measurement, the change in the luminance upon use of an 8-bit resolution camera sensor will be apparent in the obtained PPG signals, and there will be a need to consider the effect of reduced resolution on waveform features and differences in light color.

ACKNOWLEDGMENT

We thank Dr. Kazuteru Ryu for his cooperation during data measurement at the Kanai Hospital.

REFERENCES

[1] *World Health Statistics 2017: Monitoring Health for the SDGs*, World Health Org., Geneva, Switzerland, 2017.
[2] V. Chandrasekaran, R. Dantu, S. Jonnada, S. Thiyagaraja, and K. P. Subbu, "Cuffless differential blood pressure estimation using smart phones," *IEEE Trans. Biomed. Eng.*, vol. 60, no. 4, pp. 1080–1089, Apr. 2013.
[3] C. Free *et al.*, "The effectiveness of mobile-health technology-based health behaviour change or disease management interventions for health care consumers: A systematic review," *PLoS Med.*, vol. 10, no. 1, Jan. 2013, Art. no. e1001362.
[4] B. Martínez-Pérez, I. de la Torre-Díez, M. López-Coronado, and J. Herreros-González, "Mobile apps in cardiology," *JMIR mHealth and uHealth*, vol. 1, no. 2, pp. e1–e15, 2013.
[5] M. N. K. Boulos, A. C. Brewer, C. Karimkhani, D. B. Buller, and R. P. Dellavalle, "Mobile medical and health apps: State of the art, concerns, regulatory control and certification," *Online J Public Health Inform.*, vol. 5, no. 3, p. e229, Feb. 2014.
[6] S. R. Stoyanov, L. Hides, D. J. Kavanagh, O. Zelenko, D. Tjondronegoro, and M. Mani, "Mobile app rating scale: A new tool for assessing the quality of health mobile apps," *JMIR mHealth and uHealth*, vol. 3, no. 1, p. e27, Jan. 2015.
[7] D. Phan, L. Y. Siong, P. N. Pathirana, and A. Seneviratne, "Smartwatch: Performance evaluation for long-term heart rate monitoring," in *Proc. IEEE ISBB*, Oct. 2015, pp. 144–147.
[8] J. Andreu-Perez, C. C. Y. Poon, R. D. Merrifield, S. T. C. Wong, and G.-Z. Yang, "Big data for health," *IEEE J. Biomed. Health Inform.*, vol. 19, no. 4, pp. 1193–1208, Jul. 2015.
[9] W. Raghupathi and V. Raghupathi, "Big data analytics in healthcare: Promise and potential," *Health Inf. Sci. Syst.*, vol. 2, no. 1, p. 3, 2014.
[10] M. F. O'Rourke, A. Pauca, and X.-J. Jiang, "Pulse wave analysis," *Brit. J. Clin. Pharmacol.*, vol. 51, no. 6, pp. 507–522, Jun. 2001.
[11] J. Allen, "Photoplethysmography and its application in clinical physiological measurement," *Physiol. Meas.*, vol. 28, pp. R1–R39, Feb. 2007.
[12] K. Nakajima, T. Tamura, and H. Miike, "Monitoring of heart and respiratory rates by photoplethysmography using a digital filtering technique," *Med. Eng. Phys.*, vol. 18, pp. 365–372, Jul. 1996.

[13] A. Schäfer and J. Vagedes, "How accurate is pulse rate variability as an estimate of heart rate variability?: A review on studies comparing photoplethysmographic technology with an electrocardiogram," *Int. J. Cardiol.*, vol. 166, no. 1, pp. 15–29, Jun. 2013.
[14] S. Lu *et al.*, "Can photoplethysmography variability serve as an alternative approach to obtain heart rate variability information?" *J. Clin. Monit. Comput.*, vol. 22, no. 1, pp. 23–29, Feb. 2008.
[15] C. Scully *et al.*, "Physiological parameter monitoring from optical recordings with a mobile phone," *IEEE Trans. Biomed. Eng.*, vol. 59, no. 2, pp. 303–306, Feb. 2012.
[16] C. C. Y. Poon, X. F. Teng, Y. M. Wong, C. Zhang, and Y. T. Zhang, "Changes in the photoplethysmogram waveform after exercise," in *Proc. IEEE EMBS ISSS-MDBS*, Jun./Jul. 2004, pp. 115–118.
[17] A. Choi and H. Shin, "Photoplethysmography sampling frequency: Pilot assessment of how low can we go to analyze pulse rate variability with reliability?" *Physiol. Meas.*, vol. 38, no. 3, pp. 586–600, Mar. 2017.
[18] K. Takazawa *et al.*, "Assessment of vasoactive agents and vascular aging by the second derivative of photoplethysmogram waveform," *Hypertension*, vol. 32, no. 2, pp. 365–370, 1998.
[19] X.-R. Ding, Y.-T. Zhang, J. Liu, W.-X. Dai, and H. K. Tsang, "Continuous cuffless blood pressure estimation using pulse transit time and photoplethysmogram intensity ratio," *IEEE Trans. Biomed. Eng.*, vol. 63, no. 5, pp. 964–972, May 2016.
[20] D. Fujita, A. Suzuki, and K. Ryu, "PPG-based systolic blood pressure estimation method using PLS and level-crossing feature," *Appl. Sci.*, vol. 9, no. 2, p. e304, Jan. 2019.
[21] M. Elgendi, "On the analysis of fingertip photoplethysmogram signals," *Current Cardiol. Rev.*, vol. 8, no. 1, pp. 14–25, Feb. 2012.
[22] L. Wang, E. Pickwell-MacPherson Y. P. Liang, and Y. T. Zhang, "Noninvasive cardiac output estimation using a novel photoplethysmogram index," in *Proc. IEEE Eng. Med. Biol. Soc.*, Sep. 2009, pp. 1746–1749.
[23] S. C. Millasseau, R. P. Kelly, J. M. Ritter, and P. J. Chowienczyk, "Determination of age-related increases in large artery stiffness by digital pulse contour analysis," *Clin. Sci.*, vol. 103, pp. 371–377, Oct. 2002.
[24] S. R. Alty, N. Angarita-Jaimes, S. C. Millasseau, and P. J. Chowienczyk, "Predicting arterial stiffness from the digital volume pulse waveform," *IEEE Trans. Biomed. Eng.*, vol. 54, no. 12, pp. 2268–2275, Dec. 2007.
[25] I. Imanaga, H. Hara, S. Koyanagi, and K. Tanaka, "Correlation between wave components of the second derivative of plethysmogram and arterial distensibility," *Jpn. Heart J.*, vol. 39, no. 6, pp. 775–784, Nov. 1998.
[26] J. Hashimoto *et al.*, "Pulse wave velocity and the second derivative of the finger photoplethysmogram in treated hypertensive patients: Their relationship and associating factors," *J. Hypertension*, vol. 20, no. 12, pp. 2415–2422, 2002.
[27] T. Otsuka, T. Kawada, M. Katsumata, and C. Ibuki, "Utility of second derivative of the finger photoplethysmogram for the estimation of the risk of coronary heart disease in the general population," *Circulat. J.*, vol. 70, pp. 304–310, Mar. 2006.
[28] H. J. Baek, J. S. Kim, Y. S. Kim, H. B. Lee, and K. S. Park, "Second derivative of photoplethysmography for estimating vascular aging," in *Proc. 6th Int. Special Topic Conf. Inf. Technol. Appl. Biomed.*, 2007, pp. 70–72.

DAISUKE FUJITA received the M.E. degree in systems engineering from Wakayama University, Japan, in 2014, where he is currently pursuing the Ph.D. degree in systems engineering. His research interests include machine learning and biomedical data analysis.

ARATA SUZUKI received the Ph.D. degree in information science from the Nara Institute of Science and Technology, Japan, in 2006. He is currently an Associate Professor (Lecturer position) with Wakayama University. His research interests include statistical data analysis, Taguchi robust engineering, and biomedical and healthcare data analysis.